# Photoelectron studies of resonant multiphoton ionization of molecular nitrogen

S. T. Pratt, P. M. Dehmer, and J. L. Dehmer

Citation: The Journal of Chemical Physics **81**, 3444 (1984); doi: 10.1063/1.448069
View online: http://dx.doi.org/10.1063/1.448069
View Table of Contents: http://scitation.aip.org/content/aip/journal/jcp/81/8?ver=pdfcov
Published by the AIP Publishing



# Photoelectron studies of resonant multiphoton ionization of molecular nitrogen[a)]

S. T. Pratt, P. M. Dehmer, and J. L. Dehmer
*Argonne National Laboratory, Argonne, Illinois 60439*

(Received 26 April 1984; accepted 27 June 1984)

Photoelectron studies of three photon resonant, four photon ionization of $N_2$ via the $b\ ^1\Pi_u$, $v' = 0$–5, $c\ ^1\Pi_u$, $v' = 0$, 1, and $c'\ ^1\Sigma_u^+$, $v' = 0$, 1 levels are presented. A qualitative analysis of the observed photoelectron spectra in terms of homogeneous perturbations among the $b\ ^1\Pi_u$, $c\ ^1\Pi_u$, $o\ ^1\Pi_u$ states and among the $b'\ ^1\Sigma_u^+$, $c'\ ^1\Sigma_u^+$, and $e'\ ^1\Sigma_u^+$ states is partially successful. However, several of the photoelectron spectra exhibit marked deviations from the expected behavior. These deviations are discussed in terms of more complex interactions among the intermediate levels, and in terms of the dynamics of excited state photoionization. In addition, the $N_2$ $a\ ^1\Pi_g$, $v' = 0$–5 levels have been observed in two photon resonant, four photon ionization, and the results are compared with the results of earlier two-photon laser induced fluorescence studies.

## I. INTRODUCTION

Resonantly enhanced multiphoton ionization (REMPI) of molecules has been used for several years to obtain detailed spectroscopic information on the resonant intermediate state.[1] By determining the kinetic energy of the electrons ejected following REMPI, photoelectron spectroscopy (PES) can provide additional information on the branching ratios into different electronic, vibrational, and rotational levels of the product ion.[2–10] This allows one to focus directly on both the dynamics of the multiphoton process and the photoionization of excited state species. Because REMPI spectra usually exhibit well defined rotational structure, indicating that the lifetime of the intermediate level is long relative to a rotational period, it is reasonable to consider the multiphoton ionization process in two steps. In an $(m + n)$ REMPI/PES study, the excited state is prepared by $m$-photon excitation and subsequently is ionized by an additional $n$-photon process. To a first approximation, then, the photoelectron spectrum can be understood in terms of photoionization from the resonant intermediate level, and in this way new information on the photoionization of electronically excited molecules can be obtained. However, when $n$ is greater than 1, significant complications may arise in the photoelectron spectrum as a result of accidental resonances at higher intermediate levels.[10,11] This problem is avoided when the resonant intermediate level is ionized by a single photon $(n = 1)$.

In a recent paper, we presented photoelectron spectra obtained following $(3 + 1)$ ionization of $N_2$ via the $o\ ^1\Pi_u$, $v' = 1,2$ levels.[12] The $o\ ^1\Pi_u$ state is the lowest Rydberg state of $N_2$ converging to the electronically excited $A\ ^2\Pi_u$ state of $N_2^+$. It was found that more than 90% of the photoions were formed in the $A\ ^2\Pi$ state, indicating that the ion core acts as a spectator during the photoionizing transition. Since the potential curve of the $o\ ^1\Pi_u$ state is nearly identical to that of the $A\ ^2\Pi_u$ state of $N_2^+$, Franck–Condon factors for the ionizing transition strongly favor the preservation of the vibrational level of the intermediate state. Thus, not surprisingly, it was found that the photoions produced by REMPI via the $o\ ^1\Pi_u$, $v' = 1$, 2 levels are vibrationally as well as electronically state selected.

In the present paper we present an extension of this work to the study of $(3 + 1)$ ionization via the $b\ ^1\Pi_u$, $v' = 0$–5, $c\ ^1\Pi_u$, $v' = 0,1$, and $c'\ ^1\Sigma_u^+$, $v' = 0$, 1 levels. The potential energy curves relevant to this study are shown in Fig. 1. Nominally, the $b\ ^1\Pi_u$ state is a valence state, and the $c\ ^1\Pi_u$ and $c'\ ^1\Sigma_u^+$ states are the $3p\pi_u$ and $4p\sigma_u$ Rydberg states, respectively, both of which have the $N_2^+$ $X\ ^2\Sigma_g^+$ ion core.[13] However, in this spectral region the $c\ ^1\Pi_u$ and $b\ ^1\Pi_u$ states are strongly mixed by a homogeneous perturbation, as are the $c'\ ^1\Sigma_u^+$ and $b'\ ^1\Sigma_u^+$ states (the latter also nominally a valence state).[13] Recently these perturbations have been extensively analyzed at the vibronic level by Stahel *et al.*[14] This analysis is quite useful in understanding the photoelectron branching ratios from several of these strongly perturbed levels. However, in some instances the situation is compli-

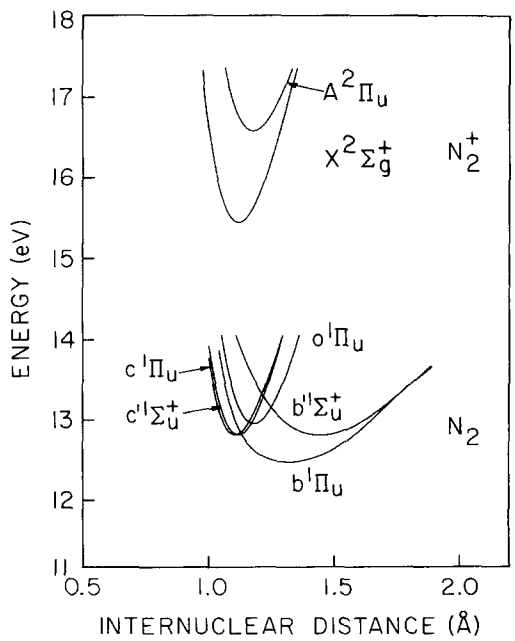


FIG. 1. Relevant potential energy curves of $N_2$ and $N_2^+$. The $N_2$ curves were generated from the deperturbed parameters of Ref. 14.

[a)] Work supported by the U. S. Department of Energy and the Office of Naval Research.

 0021-9606/84/203444-08$02.10 

cated further by strong local perturbations and predissociations which affect the rotational structure of these bands, as well as the photoelectron branching ratios, and these cases require going beyond the vibronic approximation.

## II. EXPERIMENTAL

The apparatus has been described in detail in a previous publication.[15] Briefly, it consists of a Nd:YAG pumped dye laser (Molectron MY34-10/DL18P), a time-of-flight mass spectrometer, and a hemispherical electron energy analyzer. The dye laser output was frequency doubled in a KDP crystal and the resulting UV light was separated from the fundamental by multiple reflections on dichroic beam splitters, which reduce the visible light by a factor of $10^4$. For the photoion measurements, between 0.2 and 3.0 mJ of UV light was focused into the interaction region by a plano-convex lens. The $N_2$ gas was introduced at room temperature into the interaction region by an effusive jet. The background pressure in the chamber was typically $6.5\times10^{-5}$ Torr, and the pressure at the laser focus was estimated to be 10–100 times higher. The photoion spectra were recorded by simultaneously scanning the dye laser and the KDP crystal while monitoring the $N_2^+$ ion signal. The dye laser was then tuned to the wavelength of the transition of interest and the photoelectron spectrum was recorded at the same, or somewhat lower, laser power.

A number of the photoion spectra also were recorded using a dye laser of the modified Littman design described by Mahon and Tomkins.[16] This laser incorporates two gratings and, under optimum conditions, was found to produce a bandwidth of $\sim0.05$ cm$^{-1}$, which is a factor of 6 smaller than the bandwidth of the commercial dye laser. This improvement is achieved without the necessity of pressure scanning an intracavity etalon.

In all of the measurements reported here, the photoelectron spectrometer was operated with 1 mm entrance and exit slits, and with a 2 eV energy of analysis. The resulting energy resolution was approximately 35 meV. All spectra were recorded along the polarization axis of the laser. As was described previously,[15] the transmission function of the electron spectrometer in the energy range 0.0–3.3 eV was determined by measuring the HeI photoelectron spectrum of the $O_2^+$ $b\,^4\Sigma_g^-$ and $B\,^2\Sigma_g^-$ bands under conditions identical to those used for the $N_2$ measurements. The estimated error in the relative intensities of the photoelectron peaks in the energy range 0.5–3.3 eV is $\sim30\%$. The estimated error for peaks in the energy region 0.0–0.5 eV is greater and is somewhat difficult to assess. However, peaks at energies below 0.25 eV are outside the dynamic range of the analyzer and their intensities are accurate only to within a factor of 2–3.

## III. RESULTS AND DISCUSSION

### A. Multiphoton ionization spectra

As an example of the REMPI spectra, Fig. 2 shows the spectrum of the (3 + 1) ionization of $N_2$ via the $b\,^1\Pi_u$, $v' = 5$ level. The top frame shows the REMPI spectrum obtained using the Molectron dye laser, and the bottom frame shows

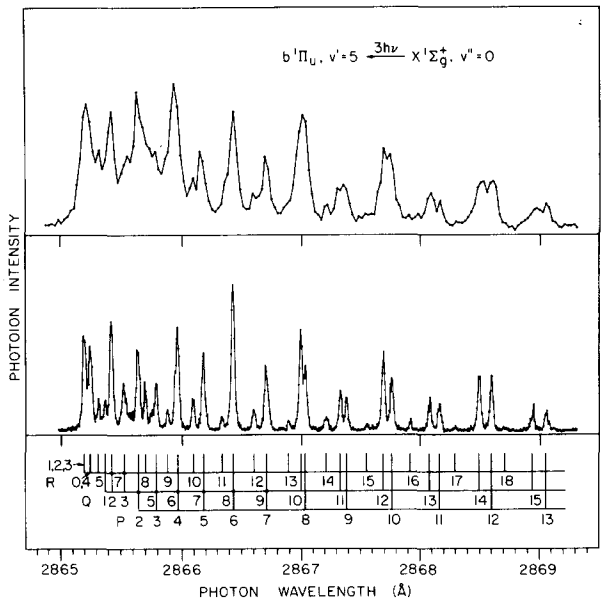


FIG. 2. The (3 + 1) ionization spectrum of $N_2$ via the $b\,^1\Pi_u$, $v' = 5$ level. The top frame shows the low resolution spectrum obtained using the commercial dye laser and the bottom frame shows the high resolution spectrum obtained using the modified Littman dye laser. Assignments are from the single photon absorption data of Ref. 17.

the REMPI spectrum of the same band obtained using the modified Littman dye laser.[16] The rotational structure is much better resolved in the latter spectrum, making the 2:1 intensity alternations in the rotational structure due to the nuclear spin statistics quite apparent.[17] Figure 3 shows the (3 + 1) ionization spectrum via the $c'\,^1\Sigma_u^+$, $v' = 0$ level. This "three headed" band has been observed previously both in absorption and in emission.[18,20] The intensity minimum in the $R$ branch between $R$ (9) and $R$ (10) is due to a strong perturbation by the $b'\,^1\Sigma_u^+$, $v = 1$ level, as is the disruption in the intensity alternation at the $P$(12) line of the $P$ branch, which is due to a blending of the $P$(11) and $P$(12) lines.[19]

The relative intensities of the observed bands show interesting variations; however, it is much more difficult to make a meaningful comparison of relative band intensities in multiphoton ionization spectra than it is in single photon absorption spectra. The intensities of the bands observed in the (3 + 1) REMPI spectra presented here depend on a num-

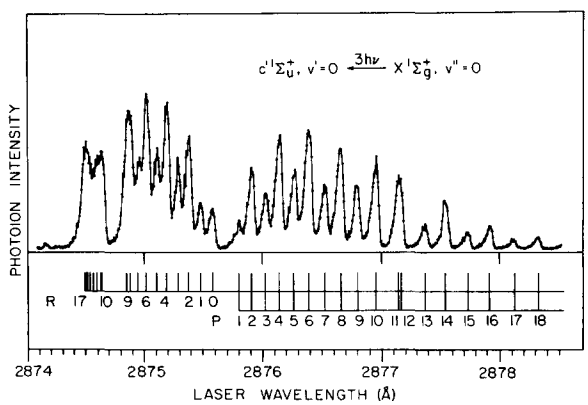


FIG. 3. High resolution, (3 + 1) ionization of $N_2$ via the $c'\,^1\Sigma_u^+$, $v' = 0$ level. Assignments are made using the data of Refs. 20 and 21.

ber of factors, including the three photon transition probabilities, and the natural lifetimes and the photoionization cross sections of the intermediate levels. Each of these quantities may display a strong dependence on the vibrational quantum number of the intermediate electronic state. For example, the three photon transition probability is proportional to

$$\left| \sum_i \sum_j \frac{\langle \Psi_f | \boldsymbol{\mu} | \Psi_j \rangle \langle \Psi_j | \boldsymbol{\mu} | \Psi_i \rangle \langle \Psi_i | \boldsymbol{\mu} | \Psi_g \rangle}{(E_j - E_g - 2h\nu)(E_i - E_g - h\nu)} \right|^2, \quad (1)$$

where $h\nu$ is the photon energy, $g$ and $f$ are the initial and final states, $E_k$ is the energy of the level $k$, and the summations are over all possible intermediate states. Not only does this transition probability depend on the overall Franck–Condon factor for the process, but it also depends on the proximity of real states to the one and two photon energies. As the energy of the three photon resonance is varied, the magnitude of the energy mismatch in the denominator also will vary. Similarly, the lifetime of the three photon state may influence the REMPI vibrational band strength as a result of predissociation. Although we will not discuss any of the band intensities in detail, one example deserves mention. A number of vibrational levels of the $b\ ^1\Pi_u$ state are predissociated to some extent,[13] with the predissociation of the $v' = 3$ level being the strongest.[13,17] Thus, it is not surprising that, although the single photon transition probability of the $b\ ^1\Pi_u$, $v' = 3 \leftarrow X\ ^1\Sigma_g^+$, $v'' = 0$ transition is intermediate between those of the (2,0) and (4,0) transitions,[14] the intensity of the (3,0) band in REMPI is much less than the intensity of either the (2,0) or (4,0) bands. Thus, predissociation effectively competes with ionization as a mechanism for depopulating the resonant intermediate level, and it is only at higher laser powers that ionization of the $b\ ^1\Pi_u$, $v' = 3$ level is observed.

In addition to the (3 + 1) ionization processes discussed above, it is also possible to observe REMPI signal due to (2 + 2) ionization of $N_2$ via the $a\ ^1\Pi_g$, $v'$ levels within the wavelength range used in this work. The $a\ ^1\Pi_g$, $v' = 0$, 1 levels have been observed previously by single photon absorption[21] and recently by two photon laser induced fluorescence.[22] Higher vibrational levels have been observed in single photon absorption, but are more difficult to detect using laser induced fluorescence due to collision-induced nonradiative transitions and to radiative transitions to other levels. However, Filseth *et al.*[23] have observed two photon transitions to the $a\ ^1\Pi_g$, $v' = 5$ level by using sensitized fluorescence with CO as the emitter. All of these bands can be observed in ionization. Figure 4 shows the $a\ ^1\Pi_g$, $v' = 5 \leftarrow X\ ^1\Sigma_g^+$, $v'' = 0$ spectrum obtained with the modified Littman dye laser. The resolution is nearly as good as that in the spectrum obtained by Filseth *et al.*[23] using a dye laser with a pressure scanned etalon. Thus, it is clear that REMPI provides an alternative for detection of excited states that might not be easily monitored in fluorescence. Although the two photon $a\ ^1\Pi_g \leftarrow X\ ^1\Sigma_g^+$ transition will not be discussed further here, we are currently using this process as the first step in double resonance experiments in an effort to probe the higher lying states of $N_2$ more precisely.

### B. REMPI/PES via perturbed intermediate levels

As was mentioned in the Introduction, the region of the

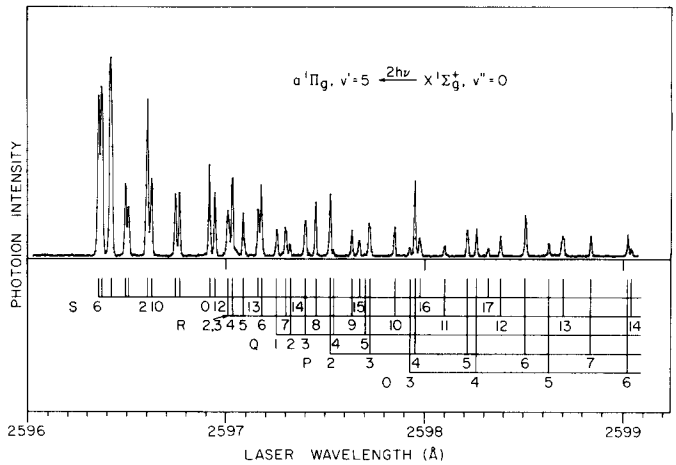


FIG. 4. The (2 + 2) ionization spectrum of $N_2$ via the $a\ ^1\Pi_g$, $v' = 5$ level. Assignments are from the single photon absorption data of Ref. 21.

$N_2$ spectrum discussed in this paper is extremely complicated, with many irregular progressions of $^1\Sigma_u^+ - X\ ^1\Sigma_g^+$ and $^1\Pi_u - X\ ^1\Sigma_g^+$ bands. This region was first analyzed by Carroll and Collins,[17] Dressler,[24] and Lefebvre-Brion,[25] and five vibrational progressions were assigned to the $b\ ^1\Pi_u$ and $b'\ ^1\Sigma_u^+$ valence states and to the $c\ ^1\Pi_u$, $o\ ^1\Pi_u$, and $c'\ ^1\Sigma_u^+$ Rydberg states. The spectrum is complicated by strong vibronic interactions among the $^1\Pi_u$ and $^1\Sigma_u^+$ states. In an extension of this earlier work, Stahel *et al.*[14] recently have presented an analysis of the $^1\Pi_u$ and $^1\Sigma_u^+$ states in terms of diabatic states and their electronic coupling energies. Their analysis provides a satisfactory fit of experimental vibronic terms, rotational $B$ values, and single photon absorption intensities. Of particular interest to the present work, their analysis provides the coefficients for expressing the observed vibronic eigenstate in terms of the diabatic states. Although strong localized perturbations in the rotational structure of these bands[13] are not reflected at the vibronic level of analysis, it is nevertheless quite useful for understanding the REMPI/PES spectra obtained in the present work.

In the analysis of Stahel *et al.*,[14] the eigenstates $\Psi$ are written as a linear combination of diabatic wave functions

$$\sum_e \sum_v c_{ev}\, \phi_e\, \chi_{ev}(R). \quad (2)$$

Here the $\phi_e$ are the diabatic electronic wave functions, the $\chi_{ev}(R)$ are the vibrational wave functions calculated in the diabatic potentials, and the $c_{ev}$ are the $R$-independent coefficients. The observed photoelectron spectrum following REMPI is then determined by the partial photoionization cross sections from the state $\Psi$ into the various vibronic continua $\Psi_{e^+v^+}\, \phi_{e^-}$, where $e^+v^+$ labels the electronic and vibrational state of the ion produced and $\phi_{e^-}$ is the continuum electronic wave function. In the Franck–Condon approximation, the partial photoionization cross section to the $e^+v^+$ state is proportional to

$$|\langle \Psi | \boldsymbol{\mu} | \Psi_{e^+v^+}\, \phi_{e^-} \rangle|^2 = \left| \sum_e \sum_v c_{ev} \langle \phi_e | \boldsymbol{\mu} | \phi_{e^+v^+}\, \phi_{e^-} \rangle \langle \chi_{ev} | \chi_{e^+v^+} \rangle \right|^2. \quad (3)$$

Although the $c_{ev}$ are known from the work of Stahel *et al.*[14] and the $\langle \chi_{ev} | \chi_{e^+v^+} \rangle$ are readily calculated, the matrix ele-

TABLE I. Dominant electronic configurations of $N_2$ and $N_2^+$ states.

| Electronic state | Configuration[a] | |
|---|---|---|
| $N_2\ X\ ^1\Sigma_g^+$ | $(1\sigma_g)^2(1\sigma_u)^2(2\sigma_g)^2(2\sigma_u)^2(1\pi_u)^4(3\sigma_g)^2$ | |
| $N_2\ b\ ^1\Pi_u$ | $(1\sigma_g)^2(1\sigma_u)^2(2\sigma_g)^2(2\sigma_u)^2(1\pi_u)^3(3\sigma_g)^1(1\pi_g)^2$<br>$(1\sigma_g)^2(1\sigma_u)^2(2\sigma_g)^2(2\sigma_u)^1(1\pi_u)^4(3\sigma_g)^2(1\pi_g)^1$ | First configuration is approximately twice as important as second |
| $N_2\ c\ ^1\Pi_u$ | $(1\sigma_g)^2(1\sigma_u)^2(2\sigma_g)^2(2\sigma_u)^2(1\pi_u)^4(3\sigma_g)^1 3p\pi_u$ | |
| $N_2\ o\ ^1\Pi_u$ | $(1\sigma_g)^2(1\sigma_u)^2(2\sigma_g)^2(2\sigma_u)^2(1\pi_u)^3(3\sigma_g)^2 3s\sigma_g$ | |
| $N_2\ b'\ ^1\Sigma_u^+$ | $(1\sigma_g)^2(1\sigma_u)^2(2\sigma_g)^2(2\sigma_u)^2(1\pi_u)^4(3\sigma_g)^1(3\sigma_u)^1$<br>$(1\sigma_g)^2(1\sigma_u)^2(2\sigma_g)^2(2\sigma_u)^2(1\pi_u)^3(3\sigma_g)^2(1\pi_g)^1$ | Configurations weighted about equally |
| $N_2\ c'\ ^1\Sigma_u^+$ | $(1\sigma_g)^2(1\sigma_u)^2(2\sigma_g)^2(2\sigma_u)^2(1\pi_u)^4(3\sigma_g)^1 4p\sigma_u$ | |
| $N_2^+\ X\ ^2\Sigma_g^+$ | $(1\sigma_g)^2(1\sigma_u)^2(2\sigma_g)^2(2\sigma_u)^2(1\pi_u)^4(3\sigma_g)^1$ | |
| $N_2^+\ A\ ^2\Pi_u$ | $(1\sigma_g)^2(1\sigma_u)^2(2\sigma_g)^2(2\sigma_u)^2(1\pi_u)^3(3\sigma_g)^2$ | |

[a] Configurations are from Refs. 13 and 28.

ments $\langle \phi_e | \boldsymbol{\mu} | \phi_{e^+v^+} \phi_{e^-} \rangle$ present two problems. First, these matrix elements depend on the kinetic energy of the ejected electron, and therefore depend on the vibrational state of the ion produced. At the relatively low kinetic energies treated here, it is probably not reasonable to assume they are independent of $v$ and $v^+$. However, in the absence of resonance phenomena it is reasonable to assume that these matrix elements will vary smoothly with $v$ and $v^+$.[26] Second, the specific form of the diabatic wave function $\phi_e$ is not uniquely defined. However, as a first approximation, it is reasonable to associate each diabatic wave function with a single electron configuration.[27] (In the case of the $b\ ^1\Pi_u$ and $b'\ ^1\Sigma_u^+$ valence states two electron configurations are considered.[28]) In addition, the $X\ ^2\Sigma_g^+$ and $A\ ^2\Pi_u$ states of $N_2^+$ are also approximated by a single electron configuration. The important configurations are given in Table I. These approximations allow one to make some qualitative predictions about the electronic matrix elements and photoelectron branching ratios. For example, photoionization from the $c\ ^1\Pi_u$ state is expected to favor the production of $N_2^+$ $X\ ^2\Sigma_g^+$, which requires a one electron transition, over the production of $N_2^+$ $A\ ^2\Pi_u$, which requires a two electron transition. Similarly, the photoionization cross sections from the $b\ ^1\Pi_u$ state to both the $X\ ^2\Sigma_g^+$ and $A\ ^2\Pi_u$ states are expected to be small, as they each require a two electron transition. How well the experimental results agree with these predictions will be discussed in the following sections.

Franck–Condon factors for the $X\ ^2\Sigma_g^+, v^+ \leftarrow b\ ^1\Pi_u, v'$, $X\ ^2\Sigma_g^+, v^+ \leftarrow c\ ^1\Pi_u, v'$ and $X\ ^2\Sigma_g^+, v^+ \leftarrow c'\ ^1\Sigma_u^+, v'$ ionizing transitions are given in Tables II, III, and IV, respectively. The $X\ ^2\Sigma_g^+, v^+ \leftarrow c\ ^1\Pi_u, v'$ and $X\ ^2\Sigma_g^+, v^+ \leftarrow c'\ ^1\Sigma_u^+, v'$ Franck–Condon factors were calculated using Morse potentials derived from the constants of Huber and Herzberg[29] for the $X\ ^2\Sigma_g^+$ state and from the deperturbed diabatic constants of Stahel *et al.*[14] for the $c\ ^1\Pi_u$ and $c'\ ^1\Sigma_u^+$ states. Because the deperturbed $\omega_e x_e$ value for the $b\ ^1\Pi_u$ state is negative,[14] a Morse potential cannot be constructed for this state. Consequently, the $X\ ^2\Sigma_g^+, v^+ \leftarrow b\ ^1\Pi_u, v'$ Franck–Condon factors were calculated using a Morse potential for the $X\ ^2\Sigma_g^+$ state (as before) and using a numerical potential fitted to the RKR potential of Stahel *et al.*[14] for the $b\ ^1\Pi_u$ state. Numerical integration of this potential reproduces the $\Delta G_{v+1/2}$ values of Stahel *et al.*[14] to within 2 $cm^{-1}$ except for the $\Delta G_{1/2}$ value, which deviates by 9 $cm^{-1}$. This discrepancy is probably due to our improper interpolation at the bottom of the well between the RKR points for the $v = 0$ level, which results in a slight lowering of the energy for the $v = 0$ level.

The photoelectron spectra obtained at the $R$-branch bandheads of the $b\ ^1\Pi_u, v' = 0-5 \leftarrow X\ ^1\Sigma_g^+, v'' = 0$ three photon transitions are shown in Fig. 5 and the corresponding spectra for the $c\ ^1\Pi_u, v' = 0, 1 \leftarrow X\ ^1\Sigma_g^+, v'' = 0$, and $c'\ ^1\Sigma_u^+, v' = 0, 1 \leftarrow X\ ^1\Sigma_g^+$ transitions are shown in Figs. 6 and 7, respectively.

TABLE II. Franck–Condon factors for $N_2^+\ X\ ^2\Sigma_g^+, v^+ \leftarrow N_2\ b\ ^1\Pi_u, v'$.

| $X\ ^2\Sigma_g^+, v^+$ | $v' = 0$ | $v' = 1$ | $v' = 2$ | $v' = 3$ | $v' = 4$ | $v' = 5$ |
|---|---|---|---|---|---|---|
| 0 | 0.0063 | 0.0300 | 0.0733 | 0.1203 | 0.1506 | 0.1562 |
| 1 | 0.0247 | 0.0820 | 0.1262 | 0.1104 | 0.0531 | 0.0078 |
| 2 | 0.0550 | 0.1178 | 0.0935 | 0.0204 | 0.0033 | 0.0445 |
| 3 | 0.0958 | 0.1117 | 0.0264 | 0.0067 | 0.0578 | 0.0619 |
| 4 | 0.1219 | 0.0703 | 0.0002 | 0.0538 | 0.0562 | 0.0060 |
| 5 | 0.1403 | 0.0234 | 0.0285 | 0.0657 | 0.0077 | 0.0178 |
| 6 | 0.1417 | 0.0004 | 0.0665 | 0.0270 | 0.0098 | 0.0530 |

TABLE III. Franck–Condon factors for $N_2^+$ $X^2\Sigma_g^+, v^+ \leftarrow N_2$ $c\,^1\Pi_u$, $v'$.

| $X^2\Sigma_g^+, v^+$ | $v'=0$ | $v'=1$ |
|---|---|---|
| 0 | 0.9705 | 0.0293 |
| 1 | 0.0274 | 0.9258 |
| 2 | 0.0020 | 0.0398 |
| 3 | 0.0001 | 0.0048 |
| 4 | 0.0000 | 0.0002 |
| 5 | 0.0000 | 0.0000 |
| 6 | 0.0000 | 0.0000 |
| 7 | 0.0000 | 0.0000 |

### C. The $b\,^1\Pi_u$, $v'=0$–2 photoelectron spectra

According to the analysis of Stahel *et al.*[14] the $b\,^1\Pi_u$, $v'=0-2$ vibronic levels contain very little $c\,^1\Pi_u$ character, and are therefore relatively unperturbed, although the $b\,^1\Pi_u, v'=2$ level shows indication of predissociation in the region of the bandhead.[13,17] Thus, the photoelectron spectra obtained via all three levels should reflect relatively pure $b\,^1\Pi_u$ character. As is expected, photoionization from these levels populates a broad distribution of vibrational levels, in qualitative agreement with the corresponding Franck–Condon factors given in Table II. On a quantitative level, however, the agreement is rather poor. The results suggest that either a minor component of the $b\,^1\Pi_u$ wave function is responsible for the observed behavior, or that a two electron process (such as autoionization) is occurring. The latter could easily result in a breakdown of the Franck–Condon approximation. Other phenomena, such as dependence of the electronic photoionization matrix element on electron kinetic energy and internuclear distance, and a $v^+$ dependence of the photoelectron angular distributions might also contribute to the observed behavior.[8,11,30] The importance of such phenomena is difficult to assess for the present results due to the complex nature of the intermediate state.

Beginning with the $b\,^1\Pi_u$, $v=1$ photoelectron spectrum, the $A\,^2\Pi_u, v^+=0$ state of $N_2^+$ becomes energetically accessible and is observed with a large intensity, as it is in the $b\,^1\Pi_u$, $v=2$ photoelectron spectrum. Unfortunately, relative intensities in this electron kinetic energy region are not reliable, making it difficult to accurately compare the intensities of the $A\,^2\Pi_u$, $v^+=0 \leftarrow b\,^1\Pi_u$, $v'=1$ and $X^2\Sigma_g^+$, $v^+=0 \leftarrow b\,^1\Pi_u$, $v'=1$ ionizing transitions.

One final comment on the $b\,^1\Pi_u$, $v'=1$ photoelectron spectrum deserves mention. The impurity peaks at 0.26 and 0.50 eV are due to (2 + 1) ionization of $O_2$ via the $C\,^3\Pi_g$, $v'=1 \leftarrow X\,^3\Sigma_g^-$, $v''=0$ transition,[31] which occurs in the same wavelength region as the three photon $b\,^1\Pi_u$, $v'=1 \leftarrow X\,^1\Sigma_g^+$, $v''=0$ process in $N_2$. Although the $O_2^+$ signal can be discriminated against in the REMPI mass spectrum (REMPI/MS), this is not possible in the photoelectron spectrum. The REMPI/MS of this two photon resonance was studied using pure $O_2$ and found to be a broad, intense continuum as a function of wavelength. We estimate the concentration of the $O_2$ impurity in our $N_2$ sample to be 0.03%. No evidence of the $O_2$ impurity is observed in any of the other photoelectron spectra.

TABLE IV. Franck–Condon factors for $N_2^+$ $X^2\Sigma_g^+, v^+ \leftarrow N_2$ $c'\,^1\Sigma_u^+, v'$.

| $X^2\Sigma_g^+, v'$ | $v'=0$ | $v'=1$ |
|---|---|---|
| 0 | 0.9999 | 0.0001 |
| 1 | 0.0001 | 0.9998 |
| 2 | 0.0000 | 0.0001 |
| 3 | 0.0000 | 0.0001 |
| 4 | 0.0000 | 0.0000 |
| 5 | 0.0000 | 0.0000 |
| 6 | 0.0000 | 0.0000 |
| 7 | 0.0000 | 0.0000 |

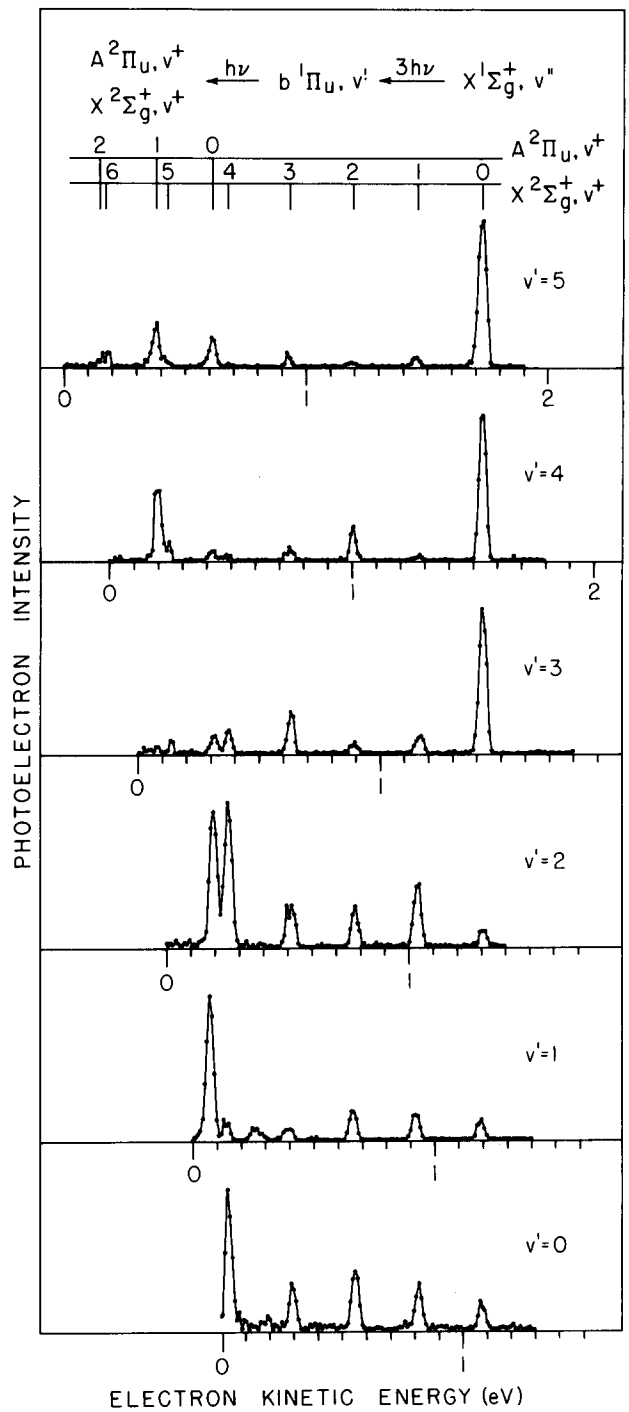


FIG. 5. Photoelectron spectra of $N_2$ following (3 + 1) ionization of $N_2$ via the $b\,^1\Pi_u$, $v'=0-5$ levels. The impurity peaks at 0.26 and 0.50 eV in the $v'=1$ spectrum are due to (2 + 1) ionization of $O_2$ and are discussed in the text.

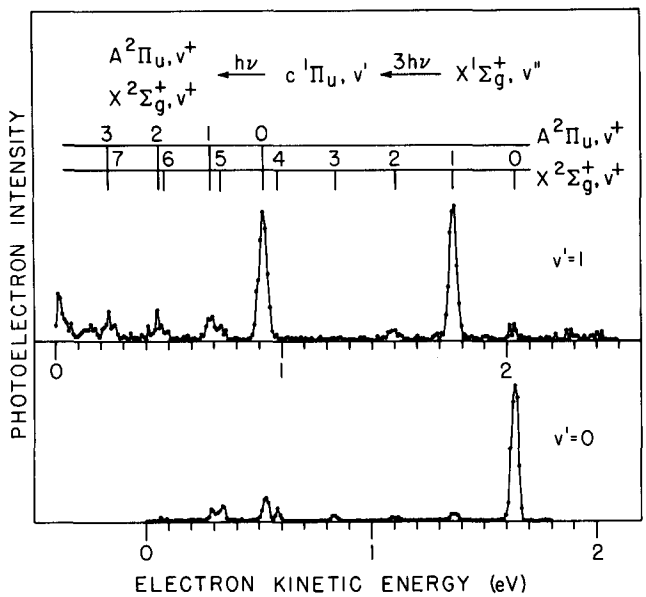


FIG. 6. Photoelectron spectra of $N_2$ following (3 + 1) ionization of $N_2$ via the $c\ ^1\Pi_u$, $v' = 0,1$ levels.

### D. The $b\ ^1\Pi_u$, $v' = 3$–5 photoelectron spectra

Unlike the $b\ ^1\Pi_u$, $v = 0-2$ photoelectron spectra, which exhibit a number of intense peaks, the $b\ ^1\Pi_u$, $v' = 3$–5 photoelectron spectra each display a single intense $v^+ = 0$ peak, with very little intensity in any of the other peaks. This is somewhat surprising since the Franck–Condon factors predict a number of other moderately intense peaks. The single intense $v^+ = 0$ peak suggests that photoionization from these levels may be dominated by a $v' = 0$ Rydberg state component in the wavefunction of the intermediate state, since photoionization from a Rydberg level is expected to preserve the vibrational quantum number of the intermediate state.[12] (This is illustrated in the photoelectron spectrum obtained following photoionization of the $c\ ^1\Pi_u$, $v' = 0$ Rydberg level, which is discussed in the following section.)

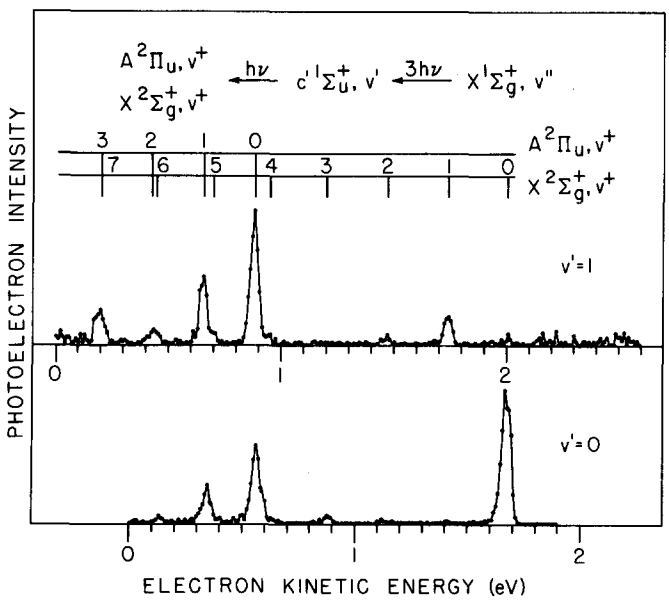


FIG. 7. Photoelectron spectra of $N_2$ following (3 + 1) ionization of $N_2$ via the $c'\ ^1\Sigma_u^+$, $v' = 0,1$ levels.

The analysis of Stahel *et al.*[14] shows that the $b\ ^1\Pi_u$, $v' = 3$–5 wave functions contain 5.8%, 16.0%, and 22.1% $c\ ^1\Pi_u$, $v' = 0$ character, respectively, and this admixture could account for the intense $v^+ = 0$ peak observed in the $b\ ^1\Pi_u$, $v' = 3$–5 photoelectron spectra. Although this qualitative argument ignores the interference terms in Eq. (3), which could lead to dramatically different behavior, the argument is a reasonable first approximation if the electronic photoionization matrix element from the $c\ ^1\Pi_u$ state is much larger than that from the $b\ ^1\Pi_u$ state. The latter is not unreasonable, as photoionization from the $c\ ^1\Pi_u$ state requires only an allowed single electron transition, while photoionization from the $b\ ^1\Pi_u$ state requires a nominally forbidden two electron transition.[28] The weaker structure in the $b\ ^1\Pi_u$, $v' = 3$–5 and $c\ ^1\Pi_u$, $v' = 0$ photoelectron spectra varies with the intermediate state. A quantitative analysis of this structure would require determining the electronic photoionization matrix elements and taking into account the interference effects.

As was mentioned above, a number of the $b\ ^1\Pi_u$, $v'$ levels are predissociated, the $b\ ^1\Pi_u$, $v' = 3$ levels being the most strongly affected.[13] This predissociation might be manifested in the photoelectron spectra as an increased intensity of a broad distribution of states, due to photoionization during the predissociation process. However, the present spectra show no evidence for such an effect, which may indicate a small photoionization cross section for the state causing the predissociation. In the present case, that state is thought to be the $C'\ ^3\Pi_u$ state,[32] which dissociates to $N(^2D^0) + N(^4S^0)$. If one ascribes the small intensity of the $N_2$ $b\ ^1\Pi_u$, $v' = 3$ REMPI spectrum to competition by predissociation, one would expect a substantial concentration of $^2D^0$ and $^4S^0$ N atoms in the laser focus. Subsequent nonresonant ionization of the N $^2D^0$ atoms requires three of the present laser photons, while ionization of the N $^4S^0$ atoms requires four.[33] The photoelectron peak corresponding to nonresonant ionization of N $^2D^0$ is calculated to occur at 0.60 eV in the $b\ ^1\Pi_u$, $v' = 3$ spectrum; however, no evidence for it is observed. Further studies are planned to attempt resonant multiphoton ionization of the $^2D^0$ and $^4S^0$ N atoms using a second tunable laser.

### E. The $c\ ^1\Pi_u$, $v' = 0,1$ and $c'\ ^1\Sigma_u^+$, $v' = 0, 1$ photoelectron spectra

While the $c\ ^1\Pi_u$, $v' = 0$ photoelectron spectrum shown in Fig. 6 can be understood by assuming that photoionization from a Rydberg level preserves the vibrational quantum number and the electronic state of the ion core, the $c\ ^1\Pi_u$, $v' = 1$ photoelectron spectrum cannot be viewed in this way. Although the latter spectrum does display a prominant $N_2^+$ $X\ ^2\Sigma_g^+$, $v^+ = 1$ peak, the $A\ ^2\Pi_u$, $v^+ = 0$ peak is equally intense. Production of the $A\ ^2\Pi_u$ electronic state from the $c\ ^1\Pi_u$ state requires a two electron transition. The appearance of the strong $A\ ^2\Pi_u$, $v^+ = 0$ peak can be rationalized by the existence of 7% $o\ ^2\Pi_u$, $v' = 0$ state character in the $c\ ^1\Pi_u$, $v' = 1$ wave function.[14] Similarly, the appearance of the $A\ ^2\Pi_u$, $v^+ = 1$ peak in the photoelectron spectrum may be due to the existence of 2% $o\ ^2\Pi_u$, $v' = 1$ character in the $c\ ^1\Pi_u$, $v' = 1$ wave function. However, the large relative in-

tensity of the $A\,^2\Pi_u$ peaks with respect to the $X\,^2\Sigma_g^+$ peaks is more difficult to understand, unless, the $A\,^2\Pi_u \leftarrow o\,^1\Pi_u$ electronic matrix element is very much larger than the $X\,^2\Sigma_g^+ \leftarrow c\,^1\Pi_u$ matrix element. It should be noted that if the $A\,^2\Pi_u \leftarrow c\,^1\Pi_u$ and $X\,^2\Sigma_g^+ \leftarrow o\,^1\Pi_u$ electronic transition matrix elements are very small, as is quite likely, the interference terms in Eq. (3) will become unimportant.

The photoelectron spectra obtained at the $R$-branch bandheads of the $c'\,^1\Sigma_u^+$, $v' = 0,1 \leftarrow X\,^1\Sigma_g^+$, $v'' = 0$ three photon transitions shown in Fig. 7 are more difficult to explain. While the $X\,^2\Sigma_g^+$, $v^+ = 0$ peak is the most intense in the $v' = 0$ photoelectron spectrum (in agreement with the Franck–Condon factors of Table IV), the $A\,^2\Pi_u$, $v^+ = 0,1$ photoelectron peaks are much larger than expected for photoionization from a Rydberg state converging to the $X\,^2\Sigma_g^+$ state of $N_2^+$. This indicates that the $c'\,^1\Sigma_u^+$, $v' = 0$ Rydberg state ion core does not act like a spectator in the ionizing transition as it did in the $o\,^1\Pi_u$ studies reported previously.[12] The $c'\,^1\Sigma_u^+$, $v' = 1$ photoelectron spectrum in Fig. 7 is even more intriguing, as the $X\,^2\Sigma_g^+$, $v^+ = 1$ peak is completely overshadowed by the intense $A\,^2\Pi_u$, $v^+ = 0, 1$ peaks. Unlike the $b\,^1\Pi_u$, $v' = 1,2$ photoelectron spectra, the strong $A\,^2\Pi_u$ peaks in Fig. 7 occur at kinetic energies for which the transmission function of the electron spectrometer is rather well known.

According to the analysis of Stahel *et al.*,[14] the $c'\,^1\Sigma_u^+$, $v' = 1$ level contains 14% $b\,^1\Sigma_u^+$, $v' = 4$ character and 2% $b'\,^1\Sigma_u^+$, $v' = 3$ character, while the $c'\,^1\Sigma_u^+$, $v' = 0$ state contains less than 2% total $b'\,^1\Sigma_u^+$ character. A large $A\,^2\Pi_u \leftarrow b'\,^1\Sigma_u^+$ electronic transition matrix element would help account for the strength of the $A\,^2\Pi_u$, $v^+ = 0,1$ peaks, but it is difficult to imagine that it is so much larger than the corresponding $X\,^2\Sigma_g^+ \leftarrow c'\,^1\Sigma_u^+$ matrix element. In addition, the Franck–Condon factors for the $A\,^2\Pi_u$, $v^+ = 1 \leftarrow b'\,^1\Sigma_u^+$, $v' = 3,4$ transitions are three and two times larger, respectively, than those for the $A\,^2\Pi_u$, $v^+ = 0 \leftarrow b'\,^1\Sigma_u^+$, $v' = 3,4$ transition, while the observed $A\,^2\Pi_u$, $v^+ = 0$ peak is nearly twice as intense as the $v^+ = 1$ peak. Thus, it does not seem likely that the explanation is so simple, and it is possible that the interference terms of Eq. (3) are important. A second possibility, which may also be applicable to the $c\,^1\Pi_u$, $v' = 1$ photoelectron spectrum, is the presence of autoionizing resonances at the four photon energy. Although two mechanisms can be postulated for the autoionization process, each has its difficulties in accounting for the observed branching ratios. Vibrational autoionization of Rydberg states converging to higher vibrational levels of the $N_2^+$ $A\,^2\Pi_u$ state is expected to favor the production of very low kinetic energy electrons,[34] and hence should not produce intense $A\,^2\Pi_u$, $v^+ = 0,1$ peaks, and weak $v^+ = 3$ and $v^+ = 4$ peaks. Similarly, electronic autoionization of Rydberg states converging to higher energy electronic states of $N_2^+$ would be expected to populate both the $A\,^2\Pi_u$ and $X\,^2\Sigma_g^+$ states, whereas in the spectrum of Fig. 7 nearly all of the intensity is in the $A\,^2\Pi_u$ state. This is not to rule out the possibility that vibrational of electronic autoionization do occur. Recent theoretical work by Giusti-Suzor and Jungen[35] on autoionization in NO indicates that the interaction of these two processes can lead to unexpected behavior in the vibrational branching ratios following autoionization. In an effort to examine this possibility, we have obtained the photoelectron spectrum from the $c'\,^1\Sigma_u^+$, $v' = 1$ state prepared by a two step process. The first laser pumped a two photon transition to the $a\,^1\Pi_g$, $v = 1$, $J = 4$ level, and a second laser was tuned to the wavelength of the $c'\,^1\Sigma_u^+$, $v' = 1$, $J' = 5 \leftarrow a\,^1\Pi_g$, $v'' = 1$, $J'' = 4$ transition. Ionization occurred by absorption of one photon of the first laser wavelength. Although the total energy is 140 $cm^{-1}$ removed from the four photon energy in the single laser experiments, the photoelectron spectrum obtained is nearly identical to that of Fig. 7. This observation indicates that the observed branching ratios are not due to sharp autoionizing resonances, although the effects of a broad autoionizing resonance cannot be ruled out. More complete studies using a second tunable laser for the ionization step are needed to determine if autoionizing resonances are present at the four photon energy. Result from single photon ionization studies[36] on $N_2$ are not applicable as they apply to the opposite parity electronic continuum.

Finally, it is worth mentioning the possibility that different photoelectron angular distributions for the $A\,^2\Pi_u$ and $X\,^2\Sigma_g^+$ states result in different intensities for these photoelectron peaks at the observation angle. Although ionization from the $c'\,^1\Sigma_u^+$ state occurs via a single photon transition, the three photon $c'\,^1\Sigma_u^+ \leftarrow X\,^1\Sigma_g^+$ transition may lead to alignment of the intermediate level. The photoelectron angular distribution then has the general form[37]

$$d\sigma/d\Omega = k \sum_{i=0}^{4} a_i \cos^{2i}\theta, \tag{4}$$

where $k$ is a constant, the $a_i$ are factors that depend on the physics of the particular process (i.e., they depend on properties of the initial and intermediate states, the partial waves of the ejected electrons, etc.) and $\theta$ is the angle between the polarization axis of the light and the direction of the ejected photoelectron. Consequently, there is no single "magic angle" at which the photoelectron spectrum can be determined to directly provide the partial cross sections. Although we have not measured the angular distributions here, measurements of the photoelectron angular distributions of other molecules following REMPI have so far shown only relatively small effects due to alignment of the intermediate level,[6,8,11] with all of the angular distributions peaked along the polarization axis of the light. The $c'\,^1\Sigma_u^+$, $v' = 1$ photoelectron spectrum might be explained if the $A\,^2\Pi_u$ angular distribution is strongly peaked along the polarization axis of the laser and if the $X\,^2\Sigma_g^+$ angular distribution is not peaked along this polarization axis. This would indicate something quite dramatic was occurring in the $X\,^2\Sigma_g^+ \leftarrow c'\,^1\Sigma_u^+$ photoionization dynamics.

All of the photoelectron spectra discussed in this paper so far have been obtained at the $R$-branch bandheads of the three photon transitions of interest. We have obtained a number of additional spectra via the $c'\,^1\Sigma_u^+$, $v' = 0$ level, including some obtained at rotational levels known to be strongly perturbed by $b'\,^1\Sigma_u^+$, $v' = 1$ rotational levels.[19]

Spectra obtained via the $R(9)$–$R(10)$ transitions and the $P(11)$–$P(12)$ transitions, which access the $c'\,^1\Sigma_u^+$, $v'=0$, $J'=10, 11$ levels that occur at the maximum of the $c'\,^1\Sigma_u^+$, $v'=0$–$b'\,^1\Sigma_u^+$, $v'=1$ perturbation, are very similar to the $c'\,^1\Sigma_u^+$, $v'=0$ spectrum shown in Fig. 7, and to other spectra obtained at relatively unperturbed positions in the band. The only differences in these spectra are small intensity variations in the weak $X\,^2\Sigma_g^+$, $v^+=3$–6 peaks. Therefore, it seems that the contribution of $X\,^2\Sigma_g^+ \leftarrow b'\,^1\Sigma_u^+$, $v'=1$ and $A\,^2\Pi_u \leftarrow b'\,^1\Sigma_u^+$, $v'=1$ processes to the photoionization cross section is rather small. This lack of a noticeable effect in the photoelectron spectra due to Rydberg-valence mixing was also observed in our earlier work on the $o\,^1\Pi_u$ state of $N_2$.[12] A stronger effect due to Rydberg-valence mixing was observed by White *et al.* in the $C\,^2\Pi$ state of NO;[3] however, in that study, the ionization step required two photons, which causes ambiguity due to the possibility of accidental resonances at the intermediate level. In the present case this lack of effect is interesting as the two most important configurations in electronic structure calculations of the $b'\,^1\Sigma_u^+$ state of $N_2$ differ from accessible ionic states by a single electron (see Table I).[28] Thus, in principle, photoionization from the $b'\,^1\Sigma_u^+$ state should be an allowed, single electron process. More cases of Rydberg-valence interaction obviously need to be examined before it will be possible to generalize such tendencies.

## IV. CONCLUSIONS

The photoelectron spectra obtained following $(3+1)$ ionization of $N_2$ via the $b\,^1\Pi_u$, $v'=0$–5, $c\,^1\Pi_u$, $v'=0,1$, and $c'\,^1\Sigma_u^+$, $v'=0$, 1 levels exhibit complicated structure due to perturbations of the resonant intermediate level. The vibronic analysis of the $^1\Pi_u$ and $^1\Sigma_u^+$ states of $N_2$ by Stahel *et al.*[14] provides a useful framework for understanding these photoelectron spectra by providing a breakdown of the strongly perturbed intermediate vibronic levels in terms of deperturbed diabatic states with well defined Rydberg or valence character. Thus, the strong $X\,^2\Sigma_g^+$, $v^+=0$ photoelectron peak in the spectra recorded via the valence $b\,^1\Pi_u$, $v'=3$–5 levels can be understood in terms of an admixture of $c\,^1\Pi_u$, $v'=0$ Rydberg character in the $b\,^1\Pi_u$ wave function. The admixture of valence character into a Rydberg state, however, does not appear to have as dramatic an effect. For example, an increase in the admixture of $b'\,^1\Sigma_u^+$ valence character in the wave function of the $c'\,^1\Sigma_u^+$, $v'=0$ Rydberg level does not significantly alter the observed photoelectron spectrum. This observation indicates that, in the present case, the photoionization cross section from the valence state is smaller than from the Rydberg state, at least at the UV wavelengths used in this work.

While a qualitative understanding can be developed for most of the photoelectron spectra presented here, a number of difficulties remain, most noticably in the spectra obtained via the $c\,^1\Pi_u$, $v'=1$ and $c'\,^1\Sigma_u^+$, $v'=1$ levels. A complete understanding of the observed spectra will be achieved only by an analysis that takes into account the interference terms of Eq. (3), and by a variable wavelength photoionization step to map out possible autoionization structure in the continuum.

## ACKNOWLEDGMENTS

The authors would like to thank Dr. F. Tomkins for providing us with his design for the modified Littman dye laser, and for his guidance in its use. We would also like to thank Professor K. Dressler for several helpful comments and for providing additional data from the analysis of Ref. 14.

[1] P. M. Johnson and C. E. Otis, Annu. Rev. Phys. Chem. **32**, 139 (1981).
[2] J. C. Miller and R. N. Compton, J. Chem. Phys. **75**, 22 (1981).
[3] M. G. White, M. Seaver, W. A. Chupka, and S. D. Colson, Phys. Rev. Lett. **49**, 28 (1982).
[4] J. Kimman, P. Kruit, and M. J. van der Wiel, Chem. Phys. Lett. **88**, 576 (1982).
[5] J. H. Glownia, S. J. Riley, S. D. Colson, J. C. Miller, and R. N. Compton, J. Chem. Phys. **77**, 68 (1982).
[6] Y. Achiba, K. Sato, K. Shobatake, and K. Kimura, J. Chem. Phys. **78**, 5474 (1983); K. Kimura, Adv. Chem. Phys. (in press).
[7] W. G. Wilson, K. S. Viswanathan, E. Sekreta, and J. P. Reilly, J. Phys. Chem. **88**, 672 (1984).
[8] S. L. Anderson, G. D. Kubiak, and R. N. Zare, Chem. Phys. Lett. **105**, 22 (1984).
[9] S. T. Pratt, P. M. Dehmer, and J. L. Dehmer, J. Chem. Phys. **78**, 4315 (1983).
[10] S. T. Pratt, P. M. Dehmer, and J. L. Dehmer, J. Chem. Phys. **79**, 3234 (1983).
[11] M. G. White, W. A. Chupka, M. Seaver, A. Woodward, and S. D. Colson, J. Chem. Phys. **80**, 678 (1984).
[12] S. T. Pratt, P. M. Dehmer, and J. L. Dehmer, J. Chem. Phys. **80**, 1706 (1984).
[13] See, for example, A. Lofthus and P. H. Krupenie, J. Phys. Chem. Ref. Data **6**, 113 (1977).
[14] D. Stahel, M. Leoni, and K. Dressler, J. Chem. Phys. **79**, 2541 (1983).
[15] S. T. Pratt, E. D. Poliakoff, P. M. Dehmer, and J. L. Dehmer, J. Chem. Phys. **78**, 65 (1983).
[16] R. Mahon and R. S. Tomkins, IEEE J. Quant. Electron. **QE-18**, 913 (1982).
[17] P. K. Carroll and C. P. Collins, Can. J. Phys. **47**, 563 (1969).
[18] P. K. Carroll and K. Yoshino, J. Phys. B **5**, 1614 (1972); K. Yoshino and Y. Tanaka, J. Mol. Spectrosc. **66**, 219 (1977).
[19] S. G. Tilford and P. G. Wilkinson, J. Mol. Spectrosc. **12**, 231 (1964).
[20] A. Lofthus, Can. J. Phys. **35**, 216 (1957).
[21] J. T. Vanderslice, S. G. Tilford, and P. G. Wilkinson, Astrophys. J. **141**, 395 (1965).
[22] N. van Veen, P. Brewer, P. Das, and R. Bersohn, J. Chem. Phys. **77**, 4326 (1982).
[23] S. V. Filseth, R. Wallenstein, and H. Zacharias, Opt. Commun. **23**, 231 (1977).
[24] K. Dressler, Can. J. Phys. **47**, 547 (1969).
[25] H. Lefebvre-Brion, Can. J. Phys. **47**, 541 (1969).
[26] J. L. Dehmer, D. Dill, and A. C. Parr, in *Photophysics and Photochemistry in the Vacuum Ultraviolet*, edited by S. P. McGlynn, G. Findlay, and R. H. Huebner (Reidel, Dordrecht, 1984), and references therein.
[27] See, for example, H. Lefebvre-Brion, in *Atoms, Molecules, and Lasers* (International Atomic Energy Agency, Vienna, 1974), p. 411.
[28] H. H. Michels, Adv. Chem. Phys. **45**, 225 (1981).
[29] K. P. Huber and G. Herzberg, *Molecular Spectra and Molecular Structure. IV* (Van Nostrand Reinhold, New York, 1979).
[30] S. T. Pratt, P. M. Dehmer, and J. L. Dehmer, Chem. Phys. Lett. **105**, 28 (1984).
[31] See, for example, T. A. York and J. Comer, J. Phys. B **16**, 3627 (1983).
[32] M. Leoni and K. Dressler, Z. Angew. Math. Phys. **22**, 794 (1971).
[33] C. E. Moore, Natl. Bur. Stand. Circ. 467, Vol. I, 1949.
[34] R. S. Berry, J. Chem. Phys. **45**, 1228 (1966); J. N. Bardsley, Chem. Phys. Lett. **1**, 229 (1967).
[35] A. Giusti-Suzor and Ch. Jungen, J. Chem. Phys. **80**, 986 (1984); see also, M. Raoult and Ch. Jungen, *ibid.* **74**, 3388 (1981).
[36] P. M. Dehmer, P. J. Miller, and W. A. Chupka, J. Chem. Phys. **80**, 1030 (1984).
[37] See, for example, P. Lambropoulos, Adv. At. Mol. Phys. **12**, 87 (1976), and references therein.